Spectroscopic and structural studies on volatile gallium β-diketonates as potential precursors for MOCVD

B. Ballarin, G.A. Battiston, F. Benetollo, R. Gerbasi and M. Porchia*
CNR, Institute of Chemistry and Inorganic Technologies and of Advanced Materials, Corso Stati Uniti 4, I-35020 Padua (Italy)

D. Favretto and P. Traldi
CNR, Area della Ricerca di Padova, Corso Stati Uniti 4, I-25020 Padua (Italy)

(Received July 19, 1993; revised October 1, 1993)

Abstract

The complexes $Ga(hfac)_3$ (Hhfac = hexafluoroacetylacetone) and $Ga(dpm)_3$ (Hdpm = dipivaloylmethane) have been studied by solid and gas phase IR, mass spectrometry, ^1H and ^{13}C NMR, in order to prove their suitability as precursors for Ga_2O_3 deposition via metalorganic chemical vapor deposition (MOCVD). The crystal structure of $Ga(hfac)_3$ was also determined. The complex crystallizes in the monoclinic space group $P2_1/n$ with $a = 9.034(3)$, $b = 13.399(3)$, $c = 19.100(4)$ Å, $\beta = 92.19(3)°$ for $Z = 4$. The final R factor was 0.048. The Ga(III) ion exhibits a regular octahedral coordination with Ga–O bond distance of 1.954(5) Å (av. value). The X-ray, IR and MS studies showed the presence of identical monomeric species both in the solid and in the gas phase. $Ga(hfac)_3$ was used in preliminary MOCVD experiments to grow Ga_2O_3 films.

Key words: Crystal structures; Gallium complexes; Bidentate ligand complexes; Chelate complexes

Introduction

Many metal oxides have been shown to function as efficient O_2 sensors owing to their property of becoming semiconductors at high temperature. Gallium oxide, Ga_2O_3, is especially promising in this respect since at room temperature it is an electrical insulator, but over 500 °C displays both in bulk and in thin film a conductivity that depends reversibly on the partial pressure of oxygen gas in the surrounding atmosphere [1]. In addition, Ga_2O_3 is chemically and thermally stable as well as catalytically inactive. This combination of properties has prompted several recent studies on the growth of Ga_2O_3 polycrystalline thin films to be used as oxygen-sensitive materials [2]. Although the CVD techniques offer several advantages (good film uniformity, high deposition rate, versatility, use of simple apparatus) to the best of our knowledge Ga_2O_3 thin films have so far been obtained only by physical methods such as sputtering and an investigation of its growth via MOCVD appeared worthwhile. The choice of the precursor is fundamental for the efficiency of any CVD processes, as it influences both the growth parameters and the quality of the films. Metal β-diketonates, extensively studied in the past (i.e. for metal separation by means of gas chromatography [3]), have attracted renewed attention because some of their properties (chiefly their high volatility and ease of synthesis, purification and handling) make them suitable as precursors in the chemical vapor deposition of oxides (i.e. superconducting oxides [4]).

In this work we have undertaken a detailed investigation of the infrared (IR) and mass spectra (MS) of $Ga(hfac)_3$ (**1**) and $Ga(dpm)_3$ (**2**) to verify on the basis of the chemico-physical properties their potential as precursors for Ga_2O_3 films. Studies on thermal stability and on the fragmentation of the precursors, by means of mass spectroscopy, are the first steps to gain information about the feasibility of a deposition process. The crystal structure of **1** is also reported and discussed.

Experimental

Due to the extreme hygroscopicity of $GaCl_3$, all operations were carried out in dinitrogen filled dry-boxes. $GaCl_3$ (Aldrich) was sublimed prior to use. Hhfac

*Author to whom correspondence should be addressed.

SSDI 0020-1693(93)03743-T

(Janssen) and Hdpm (Janssen) were distilled under reduced pressure. Benzene and n-hexane were dried and purified by standard procedures.

Nadpm was prepared by reaction of metallic sodium with Hdpm in n-hexane at room temperature. ^1H and ^{13}C NMR spectra were recorded on a Bruker AC 200 spectrometer (solvent: C_6D_6 or $CDCl_3$, chemical shifts relative to TMS). All mass spectrometric measurements were performed on a VG ZAB 2F mass spectrometer ($EI = 70$ eV). The metastable ion study was achieved by means of mass analyzed ion kinetic energy spectroscopy (MIKES). Gas phase IR spectra, in the range 4000–200 cm^{-1}, were recorded by a Mattson 3000 Fourier transform infrared spectrometer, at 4 cm^{-1} resolution; 100–500 scans were added to obtain adequate signal-to-noise ratio. The compound (10 mg) was loaded in a heatable gas cell with a path length of 10 cm and a total internal volume of 113 ml, fitted with NaCl windows. The sample was loaded in a nitrogen atmosphere; it was then vaporized and the spectra were recorded at steps of 10 °C, corresponding to about 5 min time intervals, from 50 to 250 °C. IR spectra in solid phase were recorded using either KBr or CsI pellets. Both $Ga(hfac)_3$ and $Ga(dpm)_3$ were identified on the basis of their melting point and by IR and ^1H NMR.

Synthesis of 1

Hhfac (2.1 ml, 15 mmol) was slowly added to a solution of $GaCl_3$ (875 mg, 5 mmol) in benzene at room temperature. The solution was refluxed with stirring for about 4 h to give a pale yellow solution. By reducing the volume, a crop of pale orange crystals of $Ga(hfac)_3$ was obtained (m.p. = 69 °C). An additional crop of product was obtained by sublimation of the residue at 38 °C, 1.2×10^{-2} mbar. A pale orange colour appears on refluxing the reaction mixture and during the sublimation; this effect has been already noticed during the synthesis of Ca, Sr and Ba fluorinated diketonates and has been attributed to partial decomposition of the ligands [5]. The total yield with respect to $GaCl_3$ was >90%.

^1H NMR (200 MHz, C_6D_6): δ 5.95 sppm. ^{13}C NMR (200 MHz, $CDCl_3$): δ 182 (q, ^2J(C–F) 37 Hz, *C*O), 92.8 (s, *C*H), 116 (q, ^1J(C–F) 285 Hz, *C*F_3) ppm. IR (ν, cm^{-1}): 1649s, 1629s, 1573m, 1548m, 1465s, 1435s, 1255br s, 1215br s, 1149s, 1112m, 817m, 674m, 599m, 592m, 529w, 480w, 396m, 362w, 322m, 250m.

Synthesis of 2

$GaCl_3$ (700 mg, 4 mmol) and freshly prepared Nadpm (2472 mg, 12 mmol) were mixed at room temperature in benzene. The suspension was stirred for about 4 h and filtered to remove the NaCl that formed quantitatively. The benzene was removed by evaporation under reduced pressure and the white residue was sublimed at 90 °C, 5×10^{-3} mbar (m.p. = 220 °C).

^1H NMR (200 MHz, C_6D_6): δ 5.81 (s, 1H), 1.20 (s, 18H). ^{13}C NMR (200 MHz, $CDCl_3$); δ 201.6 (*C*O), 89.3 (*C*H), 28.0 [C(*C*H_3)], 40.9 [*C*(CH_3)] ppm. IR (ν, cm^{-1}): 1590s, 1569s, 1522s, 1538s, 1449m, 1421s, 1384s, 1358s, 1297w, 1249m, 1226m, 1179m, 1147m, 1024w, 962w, 935w, 874m, 792m, 763w, 742w, 637m, 508m, 482m, 436w, 317w, 262m.

X-ray measurements and structure determination of 1

The crystal and refinement data for **1** are summarized in Table 1. A prismatic white crystal of dimensions $0.30 \times 0.34 \times 0.40$ mm was lodged in a Lindemann glass capillary and was mounted on a four-circle Philips PW 1100 (Febo System) diffractometer with graphite-monochromated Mo Kα radiation. The orientation matrix and preliminary unit cell dimension were determined from 25 reflections found by mounting the crystal at random varying each of the orientation angles χ and ϕ over a range of 120°, with $6 \leqslant \theta \leqslant 8°$. For the determination of precise lattice parameters, 25 strong reflections with $10 \leqslant \theta \leqslant 12°$ were considered. Integrated intensities for *hkl* reflections in the interval $h = \pm 11$ $k = 0 \rightarrow 16$ $l = 0 \rightarrow 15$ were measured, and two standard reflections, −3,2,4 and 1,2,7 were measured every 180 min. There were no significant fluctuations of intensities other than those expected from Poisson statistics. The intensity data were corrected for Lorentz–polarization effects and for absorption, by following the method of North *et al.* [6]; no correction was made for extinction. The structure was solved by using three-dimensional Patterson and Fourier techniques and refined with full-matrix least-squares, with anisotropic thermal parameters assigned to all the non-hydrogen atoms. The three hydrogen atoms were located by difference Fourier synthesis and refined isotropically. The function min-

TABLE 1. Crystallographic data for $Ga(hfac)_3$

Chemical formula	$C_{15}H_3F_{18}O_6Ga$
M_r	690.89
Space group	$P2_1/n$
Crystal system	monoclinic
a (Å)	9 034(3)
b (Å)	13 399(3)
c (Å)	19.100(4)
β (°)	92.19(3)
V (Å^3)	2310(1)
Z	4
T (°C)	20
D_{calc} (g cm^{-3})	1.986
λ(Mo Kα) (Å)	0.71069
R	0.048
R_w	0.052
Weighting scheme	$w = [\sigma^2(F_o) + 0.000855(F_o)^2]^{-1}$
Goodness of fit, S	1.27

imized was $\Sigma w\Delta^2$ with $\Delta = (|F_o| - |F_c|)$. Final R values were $R = 0.048$ and $R_w = 0.052$ for 1831 unique reflections. A final difference Fourier map showed maximum positive and negative peaks of 0.52 and -0.37 e Å^3, respectively. Data processing and computation were carried out by using the SHELX 76 program package [7] with atomic scattering factors taken from the International Tables for X-ray Crystallography [8] and for drawing ORTEP [9]. See also 'Supplementary material'.

MOCVD experiments

A standard horizontal, low pressure, hot wall CVD reactor of 1.5 cm diameter and 30 cm length was used. The precursor $Ga(hfac)_3$, placed in an evaporator, was transported in gas phase using nitrogen as carrier gas (100 sccm) and mixed with oxygen (100 sccm) in the reaction chamber. Total pressure, flow rate, gas phase composition and substrate temperature could all be independently adjusted. The deposition was performed on Al_2O_3 substrates.

Results and discussion

$Ga(hfac)_3$ and $Ga(dpm)_3$ complexes were obtained by reaction of $GaCl_3$ with Hhfac and Nadpm, respectively; these complexes had previously been synthesized from $Ga(NO_3)_3$ and Hhfac or Hdpm in aqueous solution [10]. $GaCl_3$ has been used as starting material for analogous complexes such as $Ga(fod)_3$ (Hfod = heptafluorodimethyloctanedione) [11] and $Ga(acac)_3$ (Hacac = acetylacetone) [12] by reaction with Hfod and Naacac, respectively. Although **1** and **2** have been known for many years and studies on their volatility and thermal behavior have already been published [10], some data are still lacking for achieving their complete characterization.

^{13}C NMR

Owing to the electron withdrawing effect of the fluorine atoms, the carbons of the CF_3 groups are highly deshielded (δ CF_3 116 ppm versus 28 ppm of C^tBu_3 in **2** and 25 ppm of CH_3 in $Ga(acac)_3$ [13] whereas the CO resonance is shifted upfield with respect to $Ga(acac)_3$ and compound **2** (δ 182 ppm versus 192 and 201 ppm). This shift may be attributed to an increased electron density on the carbon which strengthens the CO bond. The strengthening of the CO bond due to the strong negative inductive effect of the CF_3 group is evident also in the IR spectra.

Infrared spectroscopy

In order to characterize complexes **1** and **2** in the gas phase and gain preliminary information about their thermal behavior, IR studies in the gas phase at variable temperature were carried out.

The gas phase spectra, obtained in pure nitrogen atmosphere, remained unaltered up to 250 °C. Also, the solid and gas phase spectra of each compound showed the same features and peak maxima, suggesting little intermolecular interaction in the solid phase. The main vibrational groups of **1** and **2** in solid and gas phase have been assigned and the more significant data are summarized in Table 2. The region from 4000 to 1700 cm^{-1} is not included in the discussion, since the only bands observed near 3000 cm^{-1} can be attributed to C–H stretching modes.

The C=O and C=C stretching vibrations, most likely strongly mixed [14], occur for **1** at 1644 and 1623 cm^{-1}, and for **2** at 1569 and 1539 cm^{-1}. As Table 2 shows, the C=O and C=C vibrations are shifted in opposite direction with respect to those of $Ga(acac)_3$ owing to the opposite inductive effect of the fluoro-alkyl and the t-butyl groups.

In the region 1550–500 cm^{-1} skeletal modes, carbon–fluorine stretching vibrations and C–H in-plane and out-of-plane deformation vibrations of **1** overlap and mix, making the assignments difficult in the absence of a complete vibrational analysis. For compound **2**, the C–H in-plane and out-of-plane deformation can be easily identified at 1177 and 636 cm^{-1}, respectively.

In the region 500–200 cm^{-1}, four weak bands (398, 363, 323, 253 cm^{-1}) are detected in the spectrum of **1**. In this low-energy region two metal–oxygen stretching absorptions would be expected (a B_2 and an A_1 mode if related to one ring fragment, or two F_{1u} modes related to the octahedral metal–oxygens core). We assign the absorptions of 398 and 253 cm^{-1} to Ga–O stretching vibrations, the others to ring deformation vibrations [16]. In the same region, compound **2** gives rise to five bands; the more intense, at 482 and 262 cm^{-1}, can be attributed to Ga–O stretching vibrations, while the other three very weak bands, at intermediate wavenumbers may be assigned to ring deformation vibrations. In $Ga(acac)_3$, a band at 446 cm^{-1} was assigned to one of the Ga–O stretching vibrations [15]. Our results are in agreement with earlier studies on β-diketonates of different metals [3]: in general the replacement of an

TABLE 2. Selected IR bands

IR stretching modes	$Ga(hfac)_3$ (cm^{-1})	$Ga(acac)_3$ (cm^{-1})	$Ga(dpm)_3$ (cm^{-1})
ν(C=O)	1644	1600 [14]	1569
ν(C=C)	1623	1550 [14]	1539
ν(Ga–O)	398	446 [15]	482
ν(Ga–O)	253		262

TABLE 3. Fractional atomic coordinates for non-hydrogen atoms and U_{eq} ($Å^2 \times 10^3$) with e.s.d.s in parentheses for $Ga(hfac)_3$

Atom	x	y	z	U_{eq}
Ga	0.4743(1)	0.4940(1)	0.2307(1)	65.5(3)
O(1)	0.5891(5)	0.5485(4)	0.3098(3)	69(2)
O(3)	0 3632(6)	0.4355(4)	0.1516(3)	73(2)
O(5)	0.6595(6)	0.4564(4)	0.1891(3)	70(2)
O(2)	0.2871(6)	0.5296(4)	0.2743(3)	73(2)
O(4)	0.4789(6)	0.6230(4)	0.1835(3)	73(2)
O(6)	0.4677(6)	0.3658(4)	0.2806(3)	70(2)
C(1)	0.5369(9)	0.5698(6)	0.3679(5)	65(4)
C(2)	0.3895(9)	0.5783(7)	0.3833(5)	71(4)
C(3)	0.2746(9)	0.5597(6)	0.3359(5)	65(3)
C(4)	0.1163(9)	0.5781(9)	0.3580(7)	91(5)
C(5)	0.6565(10)	0.5874(9)	0.4256(5)	87(5)
C(6)	0.4181(8)	0.6436(6)	0.1256(5)	63(3)
C(7)	0.3441(11)	0.5782(8)	0.0795(5)	74(4)
C(8)	0.3268(8)	0.4777(7)	0 0965(5)	65(4)
C(9)	0.4340(11)	0.7533(7)	0.1049(7)	97(5)
C(10)	0.2559(12)	0.4098(10)	0.0427(6)	94(6)
C(11)	0.7373(9)	0.3801(6)	0.2044(4)	62(3)
C(12)	0.7050(9)	0.3056(6)	0.2508(4)	66(3)
C(13)	0.5746(9)	0.3060(6)	0.2862(4)	60(3)
C(14)	0.5496(9)	0.2238(7)	0.3405(5)	82(4)
C(15)	0.8781(9)	0.3738(8)	0.1630(5)	80(4)
F(1)	0.0200(7)	0.5269(6)	0 3218(4)	158(4)
F(2)	0.0790(7)	0.6683(5)	0.3446(5)	170(4)
F(3)	0.0970(7)	0.5618(8)	0.4211(4)	214(6)
F(4)	0.7201(7)	0.5013(6)	0.4414(4)	148(3)
F(5)	0.7640(6)	0.6446(5)	0.4039(3)	114(3)
F(6)	0.6069(6)	0.6241(6)	0.4820(3)	164(4)
F(7)	0.5671(6)	0.7824(4)	0.1076(4)	132(3)
F(8)	0.3630(10)	0.8083(5)	0.1491(5)	183(5)
F(9)	0.3785(10)	0.7737(5)	0.0456(4)	192(4)
F(10)	0.1897(9)	0.3353(6)	0.0645(4)	167(4)
F(11)	0.1487(12)	0.4489(7)	0.0088(5)	243(6)
F(12)	0.3397(10)	0.3847(9)	−0.0011(6)	223(8)
F(13)	0.6529(6)	0.1548(4)	0.3422(3)	115(3)
F(14)	0.4226(6)	0.1767(5)	0.3266(3)	131(3)
F(15)	0.5426(9)	0.2608(5)	0.4025(3)	155(4)
F(16)	0.9593(6)	0.2954(4)	0.1791(3)	118(3)
F(17)	0.8456(7)	0.3669(5)	0.0954(3)	134(3)
F(18)	0.9603(7)	0.4520(5)	0.1702(4)	139(3)

TABLE 4. Selected bond lengths (Å) and bond angles (°) with e.s.d.s in parentheses for $Ga(hfac)_3$

Ga–O(1)	1.942(5)	Ga–O(3)	1.947(6)
Ga–O(5)	1.946(5)	Ga–O(2)	1.971(5)
Ga–O(4)	1.951(5)	Ga–O(6)	1.965(5)
O–C(av.)	1.25(1)	C–C(av.)	1.38(1)
C–C(F_3)(av.)	1.52(1)	C–F(av.)	1.29(2)
O(5)–Ga–O(6)	90.8(2)	O(3)–Ga–O(4)	91.0(2)
O(1)–Ga–O(2)	91.3(2)	O(5)–Ga–O(2)	178.8(2)
O(4)–Ga–O(6)	178.5(2)	O(1)–Ga–O(3)	178.1(2)
Ga–O(1)–C(1)	124.5(5)	Ga–O(3)–C(8)	126.3(5)
Ga–O(5)–C(11)	126.3(5)	Ga–O(2)–C(3)	125.7(5)
Ga–O(4)–C(6)	126.1(5)	Ga–O(6)–C(13)	124.2(5)
C–C–F(av.)	112(1)	F–C–F(av.)	107(1)

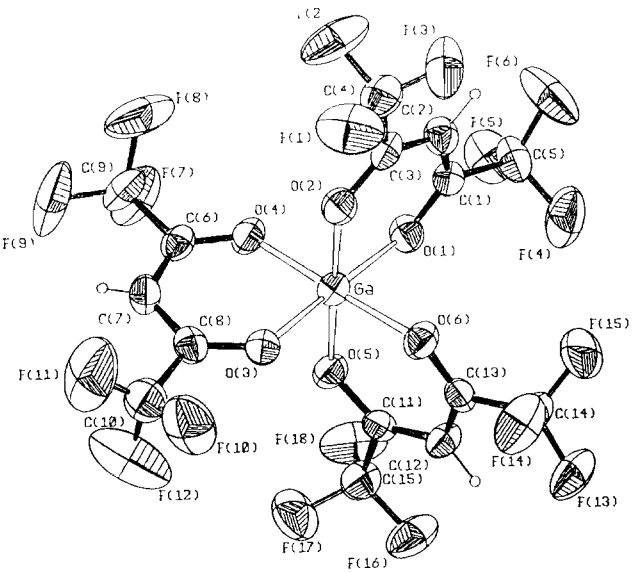

Fig. 1. ORTEP view of $Ga(hfac)_3$ with the atom-numbering scheme (the ellipsoidal boundaries are at the 30% probability level).

alkyl by a fluoro-alkyl substituent strengthens the C=O and C=C bonds and weakens the M–O bonds, causing the C=O and C=C stretching absorptions to shift to higher frequencies and M–O stretching absorption to shift to lower frequency.

Crystal structure of 1

Final fractional atomic coordinates for compound **1** are reported in Table 3. Bond lengths and angles are given in Table 4. A ORTEP view of the independent molecule with the atom-numbering scheme is given in Fig. 1. The crystal of **1** consists of well-separated $Ga(hfac)_3$ molecules. The gallium atom is octahedrally coordinated to the oxygens of the three hexafluoroacetylacetonate ligands. The Ga–O bonds lengths (ranging from 1.942(5) to 1.971(5) Å), the C–O bond distances, and the C–C distances are in agreement with the values found in the complex $Ga(acac)_3$ [12]. The 1.38 Å (av.) ring C–C bond distances show partial double bond character, consistent with the expected delocalization of π electrons in the chelate ring. The oxygen–oxygen distances, ranging from 2.712(8) to 2.794(8) Å, are similar to those found for $Ga(acac)_3$ [12].

No interaction between gallium and fluorine atoms was observed. Metal–fluorine interactions have been invoked for other hexafluoroacetylacetonates to explain the growth of metal fluoride from fluorinated precursors; an example is $[Ca(hfac)_2(H_2O)_2]_2$ for which Ca–F interactions of 2.52 Å have been found [4]. In our case the Ga–F intermolecular distances are long (2.9 Å and more) and the structure consists of a close-packet sphere

TABLE 5. 70 eV mass spectra of $Ga(hfac)_3$ and $Ga(dpm)_3$

$Ga(hfac)_3$			$Ga(dpm)_3$		
m/z	Relative abundance	Assignments	*m/z*	Relative abundance	Assignments
690	1.8	M^+	618	3.4	M^+
671	3.6	$M^+ - F$	435	77.8	$M^+ - dpm$
621	1.0	$M^+ - CF_3$	420	6.2	$M^+ - dpm - CH_3$
483	88.0	$M^+ - hfac$	405	8.7	$M^+ - dpm - 2CH_3$
464	3.7	$M^+ - hfac - F$	293	10.2	$M^+ - dpm - 2C(CH_3)_3 - CO$
433	49.4	$M^+ - hfac - CF_2$	269	6.8	$M^+ - 2dpm + OH$
414	1.0	$M^+ - hfac - CF_3$	252	6.2	$M^+ - 2dpm$
295	13.7	$M^+ - 2hfac + F$	211	8.4	$M^+ - 2dpm - C(CH_3)_3 + O$
276	8.4	$M^+ - 2hfac$	207	6.5	$M^+ - 2dpm - C(CH_3)_3 - 3CH_3$
245	15.0	$M^+ - 2hfac - CF$	195	65.7	$M^+ - 2dpm - C(CH_3)_3$
226	3.0	$M^+ - 2hfac - CF_2$	97	59.2	$GaOC^+$
69	100	CF_3^+	85	75.3	GaO^+
69	15	$^{69}Ga^+$	69	100	Ga^+

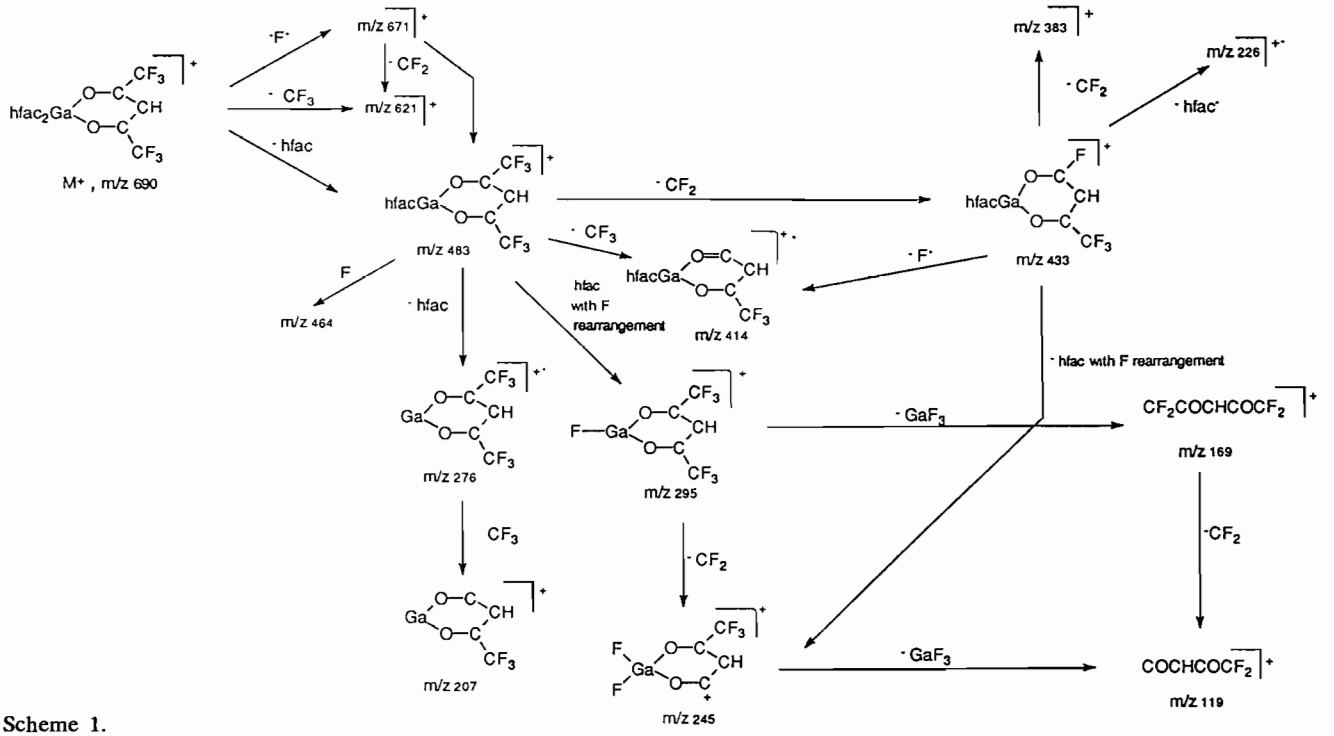

Scheme 1.

arrangement of the single molecules, in agreement with the good volatility of $Ga(hfac)_3$.

Mass spectrometry

This technique can give some important clues about the ease of ligand dissociation and about the decomposition process. The EI mass spectra of $Ga(hfac)_3$ and $Ga(dpm)_3$ are reported in Table 5; *m/z* values are calculated for ^{69}Ga.

The spectra of both complexes show extensive fragmentation, leading to fragment ions most of which contain Ga. Molecular ions are detectable for both complexes, even though not in high yield (their relative abundance is 1.8 and 3.4% for **1** and **2**, respectively).

The two decomposition pathways shown in Schemes 1 and 2 were obtained on the basis of metastable ion studies, performed by MIKES technique [17] on the molecular ions of **1** and **2**, as well as on the major fragment ions of the EI spectra. By these techniques the observed dissociation channels could be unequivocally identified.

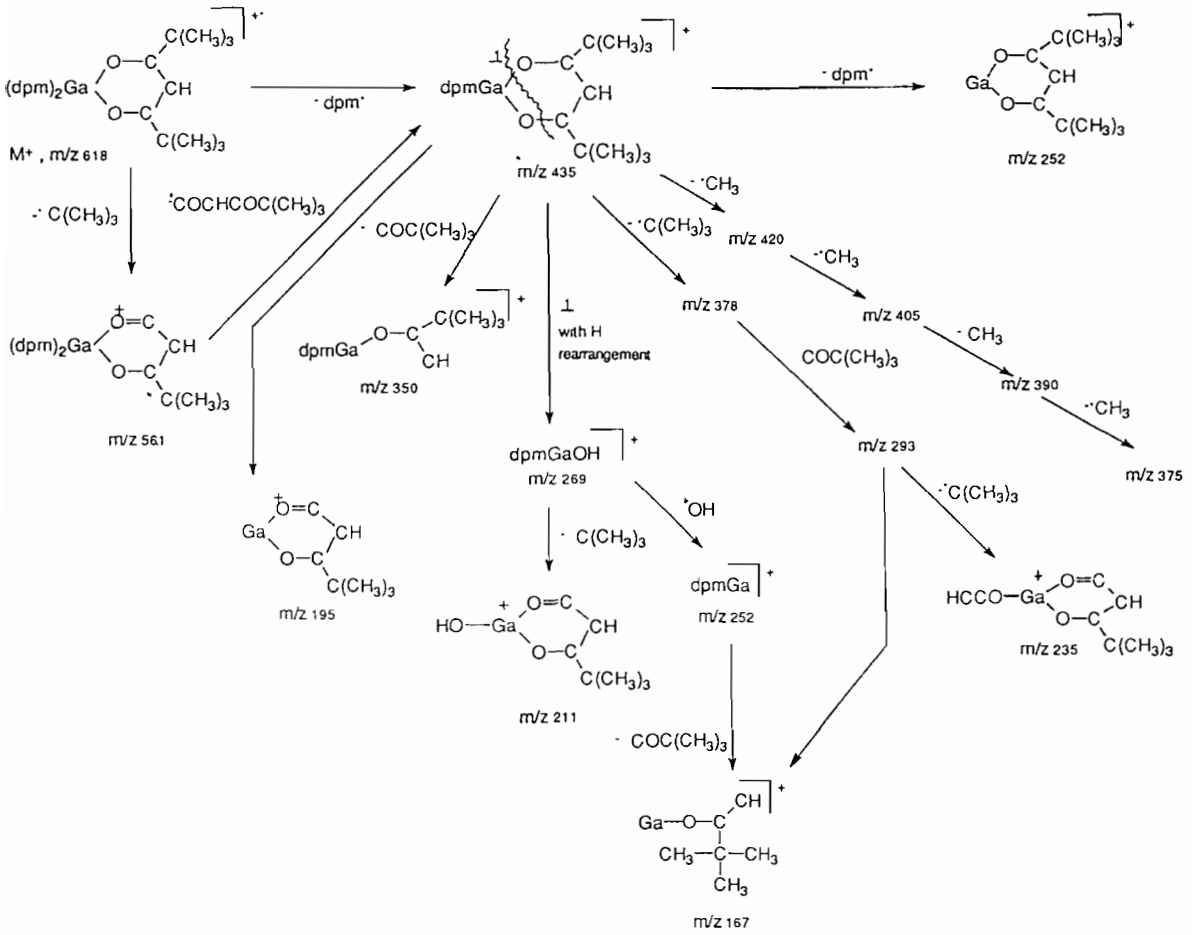

Scheme 2.

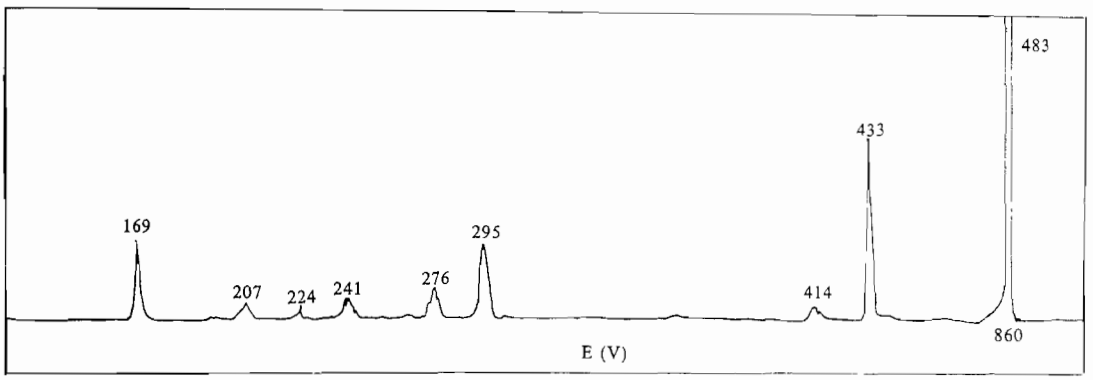

Fig. 2. MIKE spectrum of ionic species at *m/z* 483 generated by EI of $Ga(hfac)_3$.

The $M^{\cdot+}$ fragment of compound **1** shows three primary decomposition pathways consisting of the loss of F$^{\cdot}$, $CF_3^{\cdot}$ and hfac$^{\cdot}$ and leading to ions at *m/z* 671, 621 and 483, respectively. The losses of $CF_3^{\cdot}$ and hfac$^{\cdot}$ are analogous to the losses of 'But' and dpm' for compound **2**, while the loss of the highly stable F$^{\cdot}$ is favored by the availability of F atoms in the molecule.

The fragment at *m/z* 483 undergoes extensive fragmentation (see Fig. 2) involving loss of both radical species (F$^{\cdot}$, $CF_3^{\cdot}$) and neutral species (CF_2). The loss of another ligand radical occurs either with and without F rearrangement, originating ions at *m/z* 295 and 276, respectively. In the former, it is worth noting that an F–Ga bond becomes present. This kind of process has already been reported for a variety of fluorinated β-diketonate ligands and several metals other than Ga [18]; the relative extent of M–F production (M = metal) was shown to depend on the acidity of the metal site

for a given fluorinated ligand. Moreover, the formation of metal–fluorine bonds can be rationalized by considering the difference between the C–F and M–F bond energies [19], ie.e. the process should be favored when the M–F bond to be formed is as strong as, or stronger than, the C–F bond to be broken. In our case the reported mean bond energy for GaF_3 (112 Kcal/mol) [20] is comparable with that of CF_4 (116 Kcal/mol) [20], so confirming the feasability of this process. Migration of fluoride to gallium is also shown by the presence of ions at *m/z* 169 and 119, derived from ionic species at *m/z* 295 and 245 by loss of neutral GaF_3; such a decomposition route is not observed in the spectrum of $Ga(tfac)_3$ (Htfac = trifluoroacetylacetone) [21] but has been reported for other hfac complexes [3]. Whereas losses of F$^{\bullet}$ are often encountered among the decomposition routes of **1**, no loss of HF, which would necessarily involve the γ hydrogen of the ligands, is observed. This result may be considered to indicate that the γ hydrogen is less acidic in $Ga(hfac)_3$ than other metal β-diketonates for which abundant HF loss was detected [18].

For compound **2**, the only two primary fragmentation processes originating from the molecular ion at *m/z* 618, are the loss of a t-butyl radical and the highly favored loss of one entire ligand radical (dpm$^{\bullet}$) to give ions at *m/z* 561 and 435, respectively. Unlike its parent ion, the ionic species at *m/z* 435, which is one of the most abundant in the EI mass spectrum (see Table 5), fragmentates extensively as shown in Fig. 3 and Scheme 2. It has been reported [19] that the loss of an odd-electron species from an odd-electron molecular species ($M^{\bullet+}$) is favored, leading to an even elcctron fragment with no change in the oxidation state of the metal. Further elimination of odd-electron neutral species from this fragment ion will readily occur if a change in oxidation state of the metal is feasible. In our case the loss of odd-electron species (such as losses of $CH_3^{\bullet}$, dpm$^{\bullet}$, ^{t}But$^{\bullet}$) may reasonably be considered to involve reduction of the metal from Ga^{III} to Ga^{I}, accompanied by transfer of an electron from the ligand to the metal [21]. The relative stability of the oxidation state +1 for gallium is shown by the presence of the odd-electron species Gadpm$^{\bullet+}$ (*m/z* 252), and Gahfac$^{\bullet+}$ (*m/z* 276) for **1**, and even of the bare metal ion (Ga^+ *m/z* 69). Thus, the situation for the $Ga(hfac)_3$ complex is different from that of the aluminium analog, $Al(hfac)_3$ [19], for which the oxidation state +1 is not available.

In Scheme 2, the fragmentation of one ligand of the ionic species at *m/z* 435 gives ions at *m/z* 269 and 350. Cleavage 1 of Scheme 2 is especially significant; it occurs with H rearrangement, showing that the Ga–O bond does not undergo rupture. This is also confirmed by the presence of $GaOC^+$ and GaO^+ species in the EI spectrum of **2** (see Table 5).

Ga_2O_3 growth

In order to study the usefulness of the investigated compounds in MOCVD, the volatile $Ga(hfac)_3$ was tested for growing Ga_2O_3 in a conventional horizontal hot wall reactor. In preliminary deposition processes N_2 was used as carrier gas, the precursor was held at 60 °C, the growth temperature was 400–450 °C and the total pressure 26 mbar. The growths were carried on in the presence of oxygen. Electron spectroscopy chemical analysis (XPS) of the as-grown films (1–2 μm thick, dark brown and amorphous by X-ray analysis), revealed the presence of stoichiometric Ga_2O_3 with a very low content both of carbon and fluorine ($\leqslant 2\%$). After annealing at 1100 °C in air the films became white and the diffraction pattern of Ga_2O_3 (monoclinic crystal system and C_2/m space group, JCPDS 41-1103) was found [22].

These preliminary results support the feasibility of the MOCVD method for the deposition of Ga_2O_3 films

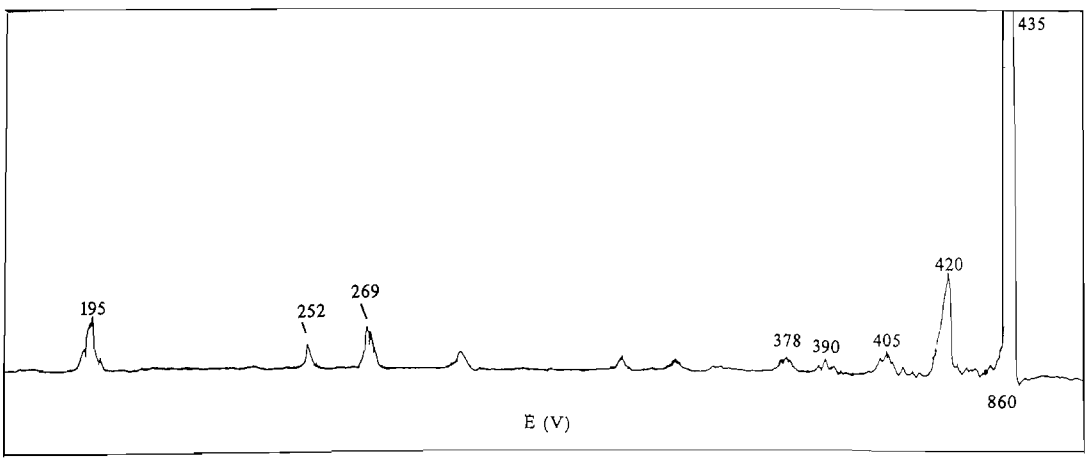

Fig. 3. MIKE spectrum of ionic species at *m/z* 435 generated by EI of $Ga(dpm)_3$.

from volatile gallium tris-β-diketonates, in agreement with our IR spectral studies and crystal data.

Supplementary material

Tables of anisotropic thermal parameters, hydrogen coordinates, complete bond lengths and angles, and a listing of calculated and observed structure factors are available from the authors on request.

Acknowledgement

The authors thank Mr L. Rizzo for technical assistance.

References

1 M. Fleischer, W. Hanrieder and H. Meixner, *Thin Solid Films, 190* (1990) 93.
2 M. Fleischer and H. Meixner, *Sensors and Actuators B, 4* (1991) 437; *6* (1992) 257.
3 R.C. Mehrotra, R. Bohra and D.P. Gaur, *Metal β-Diketonates and Allied Derivatives,* Academic Press, London, 1978.
4 L.G. Hubert-Pfalzgraf, *Appl. Organomet. Chem, 6* (1992) 627.
5 A.P. Purdy, A.D. Berry, R.T. Holm, M. Fatemi and D.K. Gaskill, *Inorg Chem., 28* (1989) 2799.
6 A.C.T. North, D.C. Phillips and F. Matheus, *Acta Crystallogr., Sect. A, 24* (1968) 351.
7 G.M. Scheldrick, *SHELX 76,* University of Cambridge, UK, 1976.
8 *International Tables for X-Ray Crystallography,* Vol. 4, Kynoch, Birmingham, UK, 2nd edn., 1974, p. 101.
9 C.K. Johnson, *ORTEP II, Rep. ORNL-5138,* Oak Ridge National Laboratory, TN, USA, 1976.
10 K. Utsunomiya, *Bull. Jpn. Chem. Soc, 44* (1971) 2688.
11 R.E. Sievers and J.W. Connolly, *Inorg. Synth., 12* (1970) 72.
12 K. Dymock and G.J. Palenik, *Acta Crystallogr., Sect. B, 30* (1974) 1364.
13 O.A. Gansow and W.D. Vernon, in G.C. Levy (ed.), *Topics in Carbon-13 NMR Spectroscopy,* Vol. 2, Wiley-Interscience, New York, 1976, Ch. 5.
14 K.E. Lawson, *Spectrochim Acta, 17* (1961) 248.
15 C. Djordjevic, *Spectrochim. Acta, 17* (1961) 448.
16 K. Nakamoto, *Infrared and Raman Spectra of Inorganic and Coordination Compounds,* Wiley-Interscience, New York, 4th edn., 1986.
17 R.G. Cooks, J.M. Beynon, R.M. Caprioli and G.R. Lester, in *Metastable Ions,* Elsevier, Amsterdam, 1973.
18 M.L. Morris and R.D. Koob, *Inorg Chem., 20* (1981) 2737.
19 C. Reichert, G.M. Bancroft and J.B. Westmore, *Can. J. Chem, 48* (1970) 1361.
20 J.E. Huheey, *Inorganic Chemistry, Principles of Structure and Reactivity,* Harper and Row, New York, 1972, Appendix f, Table F1.
21 J. Charalambous, R.G. Gossett, M.H. Johri and M.J. Kensett, *Inorg. Chim. Acta, 22* (1977) 101.
22 G.A. Battiston, R. Bertoncello, R. Gerbasi and M. Porchia, manuscript in preparation.